ROTOR CONTROL EQUIVALENT TURBULENCE INPUT (RCETI) MODELS FOR MULTI-ROTOR VEHICLES

Mahmoud A. Hayajnh **J.V.R. Prasad**

mhayajnh3@gatech.edu jvr.prasad@ae.gatech.edu

School of Aerospace Engineering
Georgia Institute of Technology
Atlanta, Georgia, USA

Abstract
This research paper aims to investigate the applicability and scalability of the Rotor Control Equivalent Turbulence Input (RCETI) models to multi-rotor vehicles. The rotor inputs and outputs are used to develop an RCETI model for the heave axis. The study begins with the development of an RCETI model for variable-RPM rotors using the rotor RPM as input and the rotor hub-load coefficient as output. Next, the input is changed to incorporate rotor collective deflections, which could be used in multi-rotor systems. Further, the effect of altering rotor parameters on the RCETI model is studied and presented in the paper. Overall, this study offers insights into the potential of the generalization of RCETI models for use in multi-rotor systems.

NOMENCLATURE

$C_{T,i}$	Thrust coefficient of rotor i
J	Fit cost function
L_w	Vertical turbulence scale length, ft
N_b	Number of rotor blades
R	Rotor radius, ft
S_x	Power Spectral Density PSD of signal x, $dB = 10log10(x)$
U_0	Mean wind speed, ft/s
V_Z	Body z-axis component of velocity, ft/s
Ω_i	Rotational speed of rotor i, percent
δ_C	Pilot collective input, percent
ω	Frequency, rad/s
σ_w	Vertical turbulence intensity, ft/s
θ_0	Swash-plate collective angle, percent
c	Blade chord length, ft
s	Laplace variable
w_g	Turbulence vertical velocity, ft/s
G	Transfer function gain, $dB = 20log10(\|G\|)$
U	Input
Y	Output
n_w	White noise source

1. INTRODUCTION

Turbulence modeling is essential for assessing the ability of an aircraft to perform certain tasks in adverse weather conditions. The highly nonlinear spatial variation of air wakes in the vicinity of buildings, ships, and other obstacles during nap-of-the-earth flight for a range of vertical lift platforms causes significant control and potential safety issues, especially during take-off and landing. These scenarios require vehicles and their control systems be designed with effective gust rejection features for safe operations in these highly complex flow environments.

The traditional approach to model turbulence for fixed-wing aircraft is done by assuming that the aircraft velocity is much higher than the turbulence velocity, and thus, a spatially frozen-field pattern of body axis gust velocities is generated from, for example, Von Karman or Dryden turbulence models[1], and are summed into the aircraft equations of motion. Although an improved approach by the implementation of complex rotating frame turbulence models [2] was found to be applicable for low speed/hover tasks, such approach is computationally expensive and can be difficult to implement in real-time simulations [3].
The notion of using control inputs that result in vehicle response that is stochastically similar to its response to atmospheric turbulence has been identified to reduce *in situ* flight testing, thus reducing risk during vehicle and its control system development. This different approach was first put forward by the National Research Council (NCR), Canada [4]. The angular rates and vertical accelerations from data of the Bell 205 hovering in turbulence were processed via a first-order inverse model of the aircraft to obtain input traces. These traces were then used as inputs to the aircraft actuators, yielding a response similar to the one measured from flight in turbulence. This notion was later extensively studied by the US Army Aeroflightdynamics Directorate (AFDD) at NASA Ames, which resulted in the development of the Control Equivalent Turbulence Input (CETI) models. In the CETI approach, the control inputs required to drive the aircraft responses to become stochastically similar to responses in actual turbulence are determined. The CETI model for the UH-60 helicopter was developed using vehicle responses from flight tests in turbulence [5]. The method was later applied to the EC135 helicopter at the German Aerospace Center (DLR) [6], showing that the approach can be applied to different aircraft. These models, however, are developed for the specific vehicles from which the data are extracted.
The lack of the existence of CETI models that can be scaled for different vehicle configurations provides motivation for developing models that can be scaled and applied for different configurations. This research builds on previous studies that developed turbulence models for specific helicopters, to develop an equivalent control input for the rotor by utilizing the hub loads as outputs, to develop the Rotor Control Equivalent Turbulence Input (RCETI) models. This recognizes that rotors are the dominant aerodynamic load-producing components at hover and low speeds. This, subsequently, reduces the parameter space in the generalization of the RCETI modeling to rotor parameters only. Previously, it has been shown that the swashplate deflections and the hub-loads can be utilized as inputs/outputs to develop the Rotor Control Equivalent Turbulence Input (RCETI) Models[7, 8]. The methodology has been carried out in the three axes (*i.e.*, vertical, longitudinal, and lateral) as Single-Input Single-Output (SISO) cases as well as coupled MIMO cases. Further, a parametric study has been done to assess the effect of the change of rotor parameters on the developed RCETI model.
The main objective of this paper is to investigate the applicability and scalability of the Rotor Control Equivalent Turbulence Input (RCETI) models to multi-rotor vehicles. The RCETI models are designed to generate rotor control inputs that produce hub-loads with spectra consistent with those induced by turbulence. The analysis focuses on the heave axis as a case study to explore the disparities between the CETI and RCETI models. Subsequently, the possibility of utilizing the same RCETI model across the rotors of a multi-rotor vehicle is explored, aiming to produce responses that are stochastically similar to the vehicle heave axis response to turbulence. The RCETI modeling is investigated for two different quadrotor configurations: one with variable-RPM and fixed-pitch, and the other with variable-pitch and fixed-RPM.
The paper is organized as follows: First, a description of the procedure for obtaining the PSDs of the CETI traces in the frequency domain is presented. Next, the suggested modeling framework for the generalization of RCETI models is described. Subsequently, the difference between the development of the CETI and the RCETI models is presented through an example. This example covers a multi-rotor vehicle that has been modeled in FLIGHTLAB® [9]. Finally, the conclusion summarizes the findings of the research and highlights the contributions and potential future work.

2. METHODOLOGY

As discussed in the introduction, developing models for turbulence simulation is a challenging task that has been the focus of extensive research. The Control Equivalent Turbulence Input (CETI) models have emerged as a valuable approach to incorporate the influence of turbulence. These models aim to capture the impact of turbulence using control inputs, enabling a direct and efficient approach to assess the response and performance of vehicles in turbulent conditions.

2.1. Control Equivalent Turbulence Input (CETI) models

The development of Control Equivalent Turbulence Input (CETI) models has been approached through various methodologies. Lusardi introduced a combined frequency and time-domain framework for the CETI model, where the measured aircraft rates were processed using an inverse of the identified aircraft model [5]. This method involved analyzing the remnant input time histories in the frequency-domain to determine the CETI model parameters. Similar approaches have been employed in other investigations [6, 10]. Recently, a frequency-domain approach was proposed and used to develop CETI models, which did not require an inverse aircraft model [11]. This approach is considered in the following discussion, and the methodology for both the SISO and the MIMO systems is described.

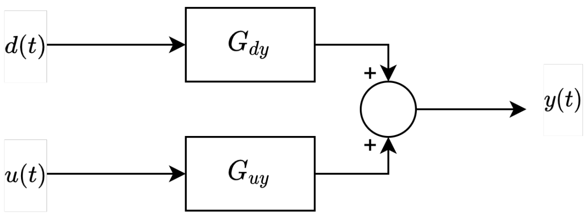

Figure 1: Vehicle response to both input and turbulence

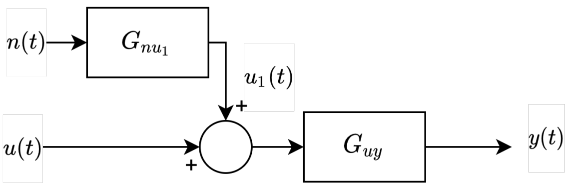

Figure 2: Block diagram of control equivalent turbulence input model.

Consider the block diagram shown in Fig. 1, the SISO equation for this diagram can be written in the frequency domain as:

$$(1) \quad Y(\omega) = G_{uy}(\omega)U(\omega) + G_{dy}(\omega)D(\omega)$$

where G_{uy} represents the aircraft frequency response to input u, and G_{dy} represents the aircraft frequency response to turbulence d.
The equation for the system with the block diagram in Fig. 2 is:

$$(2) \quad Y(\omega) = G_{uy}(\omega)[U(\omega) + U_1(\omega)]$$

where U_1 represents the remnant input that is used to account for the aircraft response to turbulence.

By rearranging Eq. 2, to solve for the remnant input U_1:

$$(3) \quad U_1(\omega) = \frac{1}{G_{uy}(\omega)} Y(\omega) - U(\omega)$$

The Power Spectral Density (PSD) of the remnant input ($S_{u_1 u_1}$) is defined as follows [12]:

$$(4) \quad S_{u_1 u_1}(\omega) = \lim_{T \to \infty} \frac{1}{T} \{U_1^* U_1\}$$

and the magnitude of the CETI transfer function model G_{nu_1} is then found when driven by a unity power white noise input as:

$$(5) \quad |G_{nu_1}| = \sqrt{S_{u_1 u_1}}$$

A CETI transfer function can then be identified via frequency domain system identification techniques such as CIFER®[13].

2.2. Rotor Control Equivalent Turbulence Input (RCETI) models

The spectra of the aircraft rates were the basis of earlier efforts to create the CETI models. In order to reduce the number of parameters for the generalization of the RCETI model, the fixed system hub-loads comprising rotor thrust, pitch moment, and roll moment may be considered. The stochastic characterization of vehicle response to turbulence is very largely driven by the stochastic characterization of rotor hub loads. Hence, the RCETI methodology is aimed at finding rotor control inputs that result in hub loads stochastically similar to those due to atmospheric turbulence (see Fig. 3). Only rotor parameters would be relevant to generalize these models since the modeling methodology is rotor-specific.

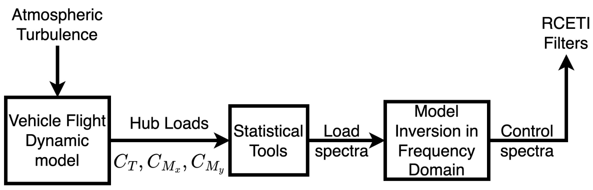

Figure 3: Rotor Control Equivalent Turbulence Input (RCETI) Modeling Framework.

For example, the spectrum of the thrust coefficient (C_T) as output due to turbulence can be measured from flight testing in turbulence. Next, an inverse mapping of the load spectrum to rotor control (Ω, for instance) spectrum can be developed. This can be found in the frequency domain by the following equation:

$$S_{\Omega}(\omega) = |\frac{C_T(\omega)}{\Omega(\omega)}|^{-2} S_{C_T}(\omega) \quad (6)$$

At this point, the RCETI models are formed by converting the control spectrum to a parametric filter transfer function via frequency domain system identification techniques using CIFER®.
The analysis can then be extended to varying rotor parameters, wherein the rotor parameters can be modified to develop different RCETI models (*i.e.*, the analysis in Fig. 3 is repeated for different rotor parameters). The effect of changing rotor parameters on the Rotor Control Equivalent Turbulence Input (RCETI) models can then be investigated. This work has been proposed and the analysis has been carried out for varying rotor parameters such as chord length, number of blades, and rotor radius [8]. A conventional single main rotor helicopter model was used in the analysis and the parameters were altered to asses the impact of change of these parameters on the shape and characteristics of the PSD of the RCETI models. Since it has been shown that the rotor is the main load-producing element of the vehicle in turbulence, this study examines the use of such models on each of the rotors in a multirotor vehicle.

3. RESULTS

In order to study the applicability of the RCETI methodology on multi-rotor vehicles, a generic quadrotor model is considered in FLIGHTLAB®. The model is described in the following section.

3.1. Quadrotor Model

The initially modeled aircraft is a fixed-pitch, variable-RPM quadrotor, which has four 3-bladed rotors in the cross-configuration as shown in Fig. 4. The model is altered in subsequent sections to study the effect of different parameters on the developed RCETI models (sections 3.7 and 3.8). For the rotors, the model features rigid blade representation and a six-state Peters-He finite state inflow model [14]. The NACA0012 airfoil was used for the blade airloads and a lookup table is used for calculating the aerodynamic forces and moments of the fuselage. The detailed specifications of the quadrotor are presented in Table 1. Due to the symmetry of the vehicle, the product moments of inertia are set to zero (*i.e.*, $I_{xy} = I_{xz} = I_{yz} = 0$).
To allow for the definition of the conventional longitudinal, lateral, collective, and pedal inputs (*i.e.*, δ_B, δ_A, δ_C, and δ_P respectively), the rotational speed inputs for each vehicle are configured as illustrated in Fig. 5. An ideal engine with no actuator dynamics is assumed (*i.e.*, the required rotational speed is achieved instantly). It is worth noting that, for this study, the configuration of the quadcopter was not optimized for flight performance. The resulting individual rotational speed of each rotor can be found as follows (in percentage):

$$\begin{bmatrix} \Omega_1 \\ \Omega_2 \\ \Omega_3 \\ \Omega_4 \end{bmatrix} = \begin{bmatrix} 1 & 1 & 1 & 1 \\ 1 & -1 & 1 & -1 \\ -1 & -1 & 1 & 1 \\ -1 & 1 & 1 & -1 \end{bmatrix} \begin{bmatrix} \delta_B \\ \delta_A \\ \delta_C \\ \delta_P \end{bmatrix} \quad (7)$$

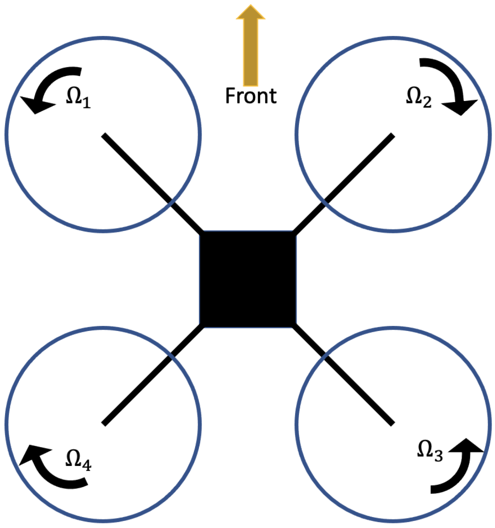

Figure 4: Quadrotor

Table 1: Quadrotor Parameters

Parameter	Value
Gross Weight	150 lbs
Rotor Radius	1 ft
Blade Chord length	0.165 ft
Boom Length	2.12 ft
Number of blades (N_b)	3
I_{xx}	10 slug-ft^2
I_{yy}	10 slug-ft^2
I_{zz}	15 slug-ft^2

3.2. Linear Time-Invariant approximations from FLIGHTLAB®

After trimming the vehicle at hover, Linear Time-Invariant (LTI) approximations are extracted from FLIGHTLAB®. These LTI approximations include body and rotor states. Different inputs and outputs

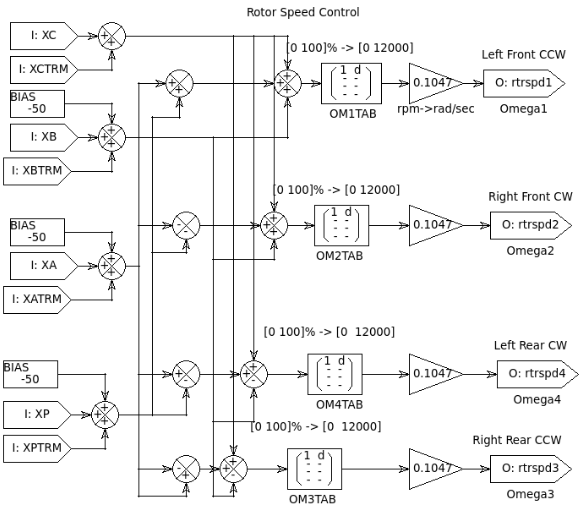

Figure 5: Schematic of the control system in FLIGHTLAB®

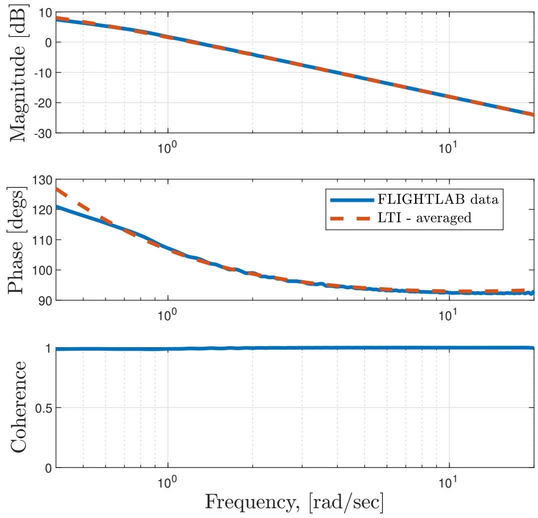

Figure 6: Frequency response of vertical velocity to collective input V_Z/δ_C

can be used. For the analysis in the following section, we consider the heave axis and thus used the vertical speed (V_Z) and the individual rotor thrust coefficients ($C_{T_i}, i = 1, 2, 3, 4$) as outputs. For the inputs of the LTI approximations, the conventional inputs (δ_B, δ_A, δ_C, and δ_P) as well as the z-axis wind speed (w_g) are used. The reason for including all of the inputs is to be able to use the matrix in Eq. 7 to find the frequency responses of outputs to the individual rotor rotational speeds ($\Omega_i, i = 1, 2, 3, 4$). The different transfer functions between inputs and outputs are then developed from the LTI approximations. These transfer functions can be used in the frequency-domain CETI/RCETI methodology to find the PSD of required inputs.

A frequency sweep input is applied to the FLIGHTLAB® non-linear model in order to validate the LTI approximations. The sweep input results are used in CIFER® to find the frequency responses. The on-axis frequency responses from CIFER® (blue line) and from the LTI approximation (dashed red line) are shown in Fig. 6. The error cost function is computed as a weighted sum of the magnitude and phase errors between the frequency response from the non-linear data and the LTI approximation response as suggested in Ref. 13. It is found that the error cost function for V_z/δ_C and C_{T_1}/δ_C are 5 and 3 respectively, suggesting that the fidelity of the extracted LTI models is good and thus, they could be utilized in the analysis.

3.3. Example of the heave axis

Our analysis starts by focusing solely on inputs and outputs along the vertical axis, which is the stable axis of the quadrotor. This is a simple example that showcases the difference between the CETI and RCETI models for multi-rotor vehicles. In this scenario, it is assumed that the turbulence fluctuations affect the entire vehicle uniformly. This assumption, albeit ambitious, maintains some validity when restricting the analysis to the vertical axis only (no moments are produced since the full vehicle is experiencing the same fluctuations). This uniform effect leads to changes in the thrust coefficients across all rotors, as well as changes in the airloads on the vehicle fuselage. As a result, the vertical acceleration of the vehicle is altered. For the turbulence model, the Dryden model is employed to simulate the effects of turbulence on the vehicle due to its simplicity. The Dryden turbulence transfer functions are given as[15]:

$$\frac{w_g}{n_w} = \frac{\sigma_w \sqrt{\frac{U_0}{\pi L_w}}(\sqrt{3}s + \frac{U_0}{L_w})}{(s + \frac{U_0}{L_w})^2} \quad (8)$$

where n_w is a unity-power white noise source. The parameters for the Dryden model are chosen as follows to represent a mild wind condition: mean wind speed of 5 knots ($U_0 = 5$ knots), turbulence intensity of 3 ft/s ($\sigma_w = 3$ ft/s), and a scale length of 10 (2 times the length of the quadrotor).

3.4. Recovering input traces

A frequency range of 1-20 rad/s is chosen for the analysis [5, 16]. In earlier studies [7, 8], a comparison has been carried out to highlight the disparity between the utilization of vehicle response and hub-loads as outputs in the analysis for a single main rotor vehicle. In addition, a comparison between utilizing the spectrum of the pilot inputs versus the swashplate inputs has been presented. It has been shown that parametric RCETI models can be developed and utilized to simulate turbulence effects on vehicles. For the analysis herein, we consider the analysis for multi-rotor vehicles. The PSD of the vehicle response as well as the hub-loads due to turbulence are found in the frequency domain directly from the transfer function matrix. In the next step, the transfer functions of the hub-loads due to rotor control inputs are used to find the PSD of the remnant input that would produce the same response spectrum produced by turbulence (using similar to Eq.6). The PSD of the vehicle collective input (δ_C) that produces similar vehicle response (V_Z) to that produced by turbulence, as well as the PSD of the rotor control input (Ω_1) that produces similar rotor thrust coefficient (C_{T_1}) to that produced by turbulence are shown in Fig. 7. Similar results for the other rotors are found. It can be observed that the spectrum of the rotational speed is similar to the spectrum of the vehicle collective input. This is expected since the actuator dynamics are neglected in this model resulting in a unity gain influence of the collective input on rotor speed. Given the context of our exploration involving quadrotors with smaller rotors that lack cyclic inputs, it is worth noting that the development of RCETI models for pitch and roll moments for each rotor is unnecessary.

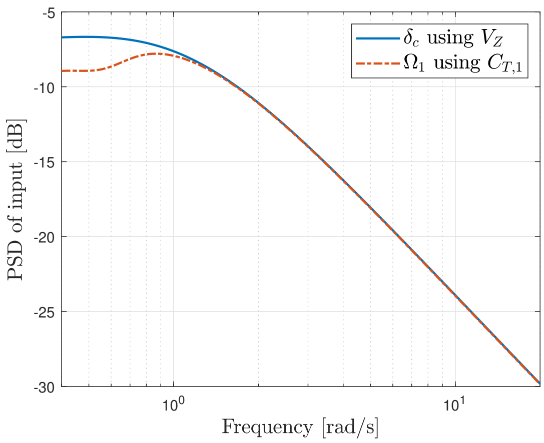

Figure 7: PSD of the input: CETI vs RCETI

3.5. Validation of the developed RCETI

It is necessary to demonstrate that the turbulence effect can be captured by utilizing rotor control inputs instead of turbulence. For this, a time-domain simulation of the vehicle is carried out in FLIGHTLAB®. It is worth noting that, since the heave axis is stable in hover, it can be simulated open loop. Both turbulence (w_g) as well as the individual rotor control inputs (Ω_i, $i = 1, 2, 3, 4$) are used. To create sample fluctuations of the vertical turbulence ($w_g(t)$), a white noise signal is used as input to the Dryden model as shown in Fig. 8. On the other hand, to create sample fluctuations of the rotational speeds, a first-order filter is developed using CIFER to reproduce the same spectrum as in Fig. 7. This filter is presented in Eq. 9, with a cost function of 14, which indicates a good match of the PSD data [13]. A white noise signal is used as an input to this filter as shown in Fig. 9, to create sample fluctuations of the rotational speeds.

$$\frac{\Omega}{n_\Omega} = \frac{0.7}{s + 1.6}, \quad J = 14 \tag{9}$$

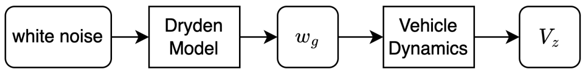

Figure 8: Time domain simulation of turbulence using Dryden model

The time history sample responses of the vertical velocity to these sample fluctuations are shown in Fig. 10. The responses are not expected to match exactly because the two simulation cases are driven by different white noise sources. However, the characteristics in terms of frequency and magnitude of the oscillations in the data do match. To validate this, the PSD of vertical velocity is determined for both simulation scenarios. In Fig. 11, the results from both cases are presented alongside analytical outcomes, demonstrating a match among the different cases.

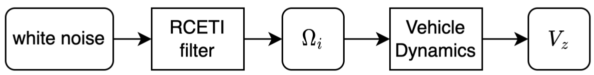

Figure 9: Time domain simulation of turbulence using RCETI model

3.6. Differential turbulence fluctuations

The primary focus of the initial analysis was to examine the vertical motion induced by uniform fluctuations across the full vehicle. The outcomes of the previous sections showed that employing RCETI models on each individual rotor yields the ability to closely replicate vertical motion responses that

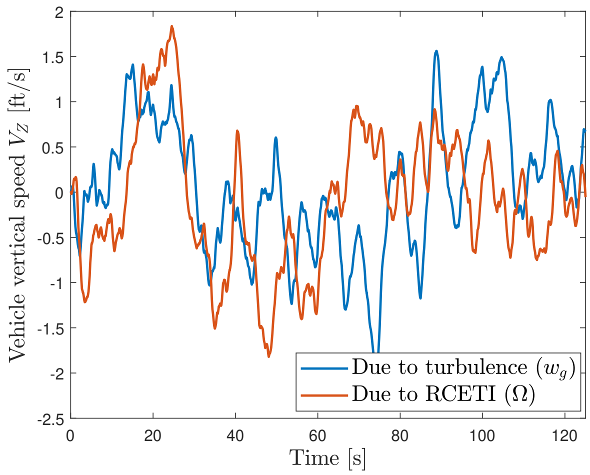

Figure 10: Heave RCETI model verification

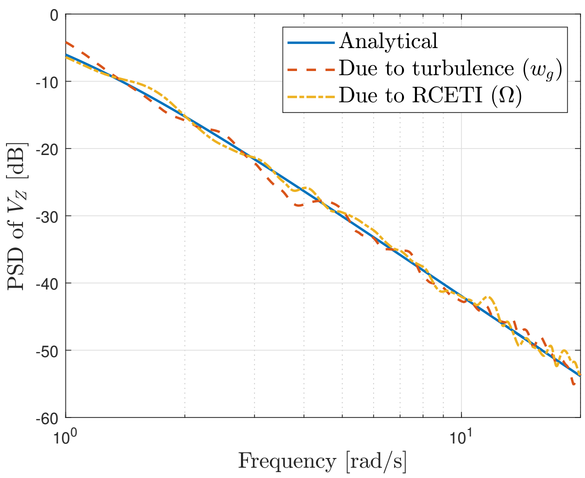

Figure 11: Heave RCETI verification in frequency domain

are stochastically similar to those arising from turbulence. This understanding serves as a foundation for extending the analysis to scenarios involving differential turbulence fluctuations across different rotors, where the resulting effects introduce moments on the vehicle and consequently vehicle rate responses.
To study this aspect, one can look into a simplified scenario where the quadrotor moves into stationary turbulence, and we apply the principles of the Taylor Hypothesis [17]. In essence, this hypothesis implies that the fluctuations experienced by the rear rotors mirror those encountered by the front rotors. However, due to spatial variations between the rotors, there exists a time delay Δt between these two sets of fluctuations. This temporal lag, Δt, is a function of the airspeed and the spatial separation between the rotors. Essentially, the delay signifies the time it takes for turbulence generated at the front rotors to propagate and affect the rear rotors. Although the Taylor Hypothesis may not fully reflect real-world conditions, we can employ it for the purpose of our simplified analysis.
To employ this concept in our simulation, the rear rotors will experience turbulence velocity with a time lag, Δt, compared to the front rotors. This time lag is given by:

$$(10)\quad \Delta t = \frac{\Delta x}{U_0}$$

where Δx is the distance between the front and rear rotors, and U_0 is the mean wind speed. Using the Dryden model, the sample fluctuations of turbulence (w_g) on the front rotors can still be found as in Fig. 8. However, a time delay should be introduced when computing the sample fluctuations for the rear rotors as shown in Fig. 12.

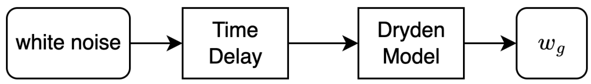

Figure 12: Delayed turbulence fluctuations on the rear rotors

Both the Dryden model and the RCETI model are employed in the simulation with similar time delays of the white noise input. For this simulation, since the vehicle is not stable except for the vertical axis, a stabilizing rate feedback controller is implemented. This controller, although not fine-tuned for the vehicle, serves the purpose of preventing instability. A segment of the sample response for the vertical velocity and the pitch rate response from both simulations is illustrated in Fig. 13. Unlike the preceding section, in this case, a pitch rate response is induced as a result of the time delay between the front and rear rotors. The sample vehicle response to turbulence exhibits a comparable magnitude and frequency to the response produced by the RCETI model, highlighting the efficacy of the RCETI model in emulating the stochastic response in this scenario. To confirm this, the PSD of the pitch rate response is computed for both simulation scenarios and the results are presented In Fig. 14, demonstrating a match among the different cases. In conclusion, this section demonstrates that the RCETI model can be effectively employed on individual rotors when subjected to different white noise inputs. The analysis highlights the ability of the RCETI model to accurately capture and replicate the response of each rotor to produce differential turbulence fluctuations, further showcasing its applicability in simulating the behavior of multi-rotor vehicles under turbulent conditions.

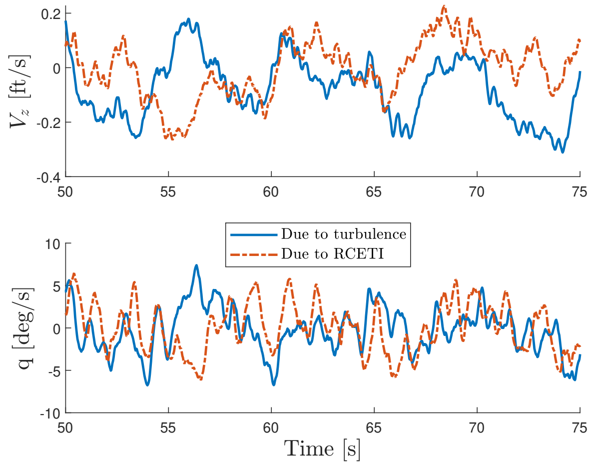

Figure 13: Time domain sample response of delayed input

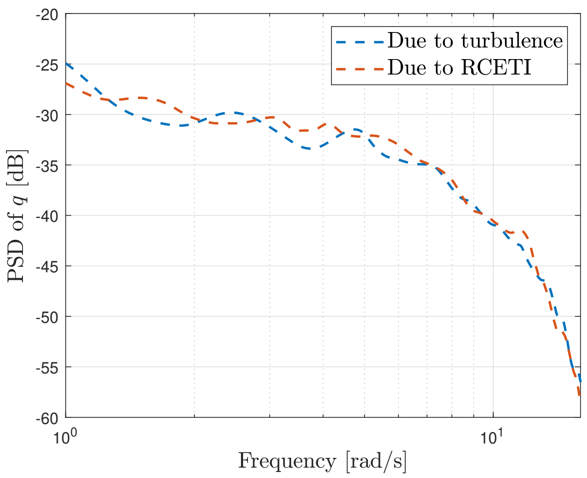

Figure 14: PSD of output

3.7. Variable-pitch rotors

Having examined the rotational speed as an input to the rotor (typically employed in multi-rotor vehicles), we shift our focus to fixed-RPM variable-pitch quadrotors. These types of rotors have garnered recent attention due to their distinct benefits compared to RPM control. One noteworthy advantage is their capability for autorotation. Furthermore, this analysis aims to facilitate a comparison with prior findings from the analysis of single main rotor vehicles. To this end, a new model is developed in FLIGHTLAB®, employing a control schematic similar to the one depicted in Fig. 5, where the modification is made to the outputs of the schematic, now representing the collective angles rather than the rotational speeds.

Similar to the analysis of the rotational speed, the PSD of the thrust coefficient due to turbulence is used to find the PSD of the collective angle (θ_0) in the frequency domain (similar to Eq. 6 with θ_0 in place of Ω). As anticipated, the utilization of the collective angles as inputs yields results similar to those obtained with rotational speed. This similarity is reflected in the discrepancy between the PSD of the pilot collective input (δ_c) and the collective angle input (θ_0), as depicted in Fig. 15, which resembles the difference observed in the case of rotational speed inputs shown in Fig. 7.

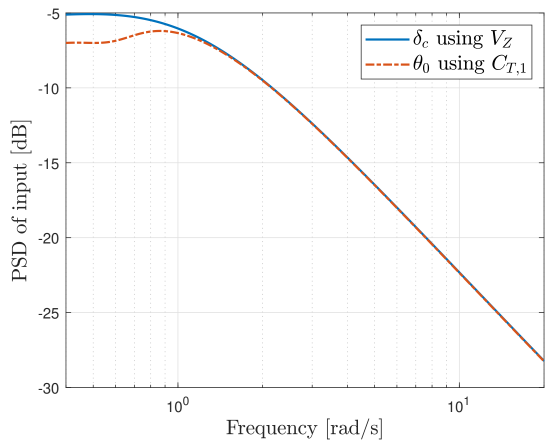

Figure 15: PSD of the input: CETI vs RCETI

3.8. Change of parameters

The analysis conducted in this section employs the variable-pitch fixed-RPM model, with adjustments applied to this particular model. Similar to the analysis in previous work [8], the parameters that are investigated in this study are as follows:

1. The vehicle weight (W).
2. The number of blades (N_b).
3. The blade chord length (c).

Changing the weight of the vehicle changes the thrust coefficient of each rotor that is required for trim under the same flight condition. To assess how changing the vehicle weight impacts the RCETI model, the weight of the vehicle is altered in FLIGHTLAB® (the nominal value is altered to 75% and 125% of the nominal value). Different Linear-Time Invariant approximations are developed and the same analysis is done to find the PSDs of the required inputs. In Fig. 16, the PSDs of the vehicle vertical velocity for different values of the weight are shown. As expected, vehicles with less weight are more susceptible to turbulence, leading to higher values of PSD of the vertical velocity. For the PSDs of the required input, similar PSDs are found for different values of the vehicle weight as shown in Fig. 17. This implies that a similar RCETI model can be used for the heave axis of similar rotors, even with different vehicle weights.

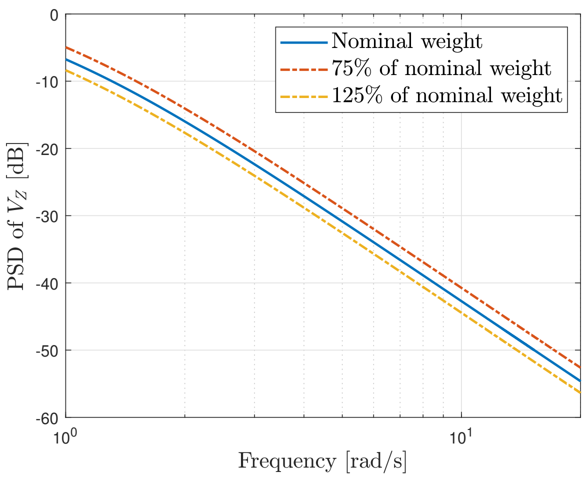

Figure 16: PSD of output: change of weight

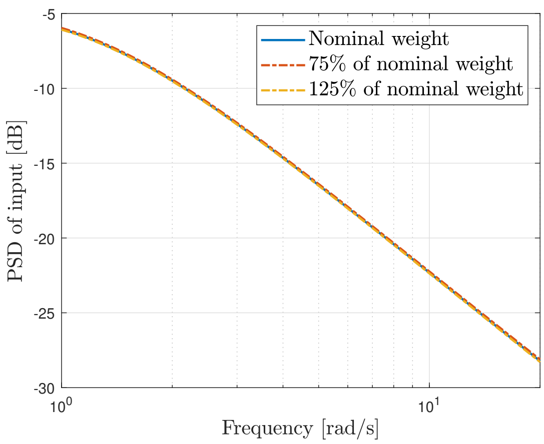

Figure 17: PSD of the input: change of weight

Next, the effect of changing the number of blades (N_b) of the rotor on the RCETI model is also considered here. To address this, transfer functions are developed for the different numbers of blades of the rotor (we consider N_b = 2 and 3, since they are commonly used in quadrotors). The PSDs of the vertical velocity in Fig. 18 show that the spectrum of V_Z increases with increasing the number of blades. This increase is anticipated since a larger area of the rotor is exposed to turbulence with more number of blades. However, this difference does not greatly alter the RCETI model since, in the case of more number of blades, the same deflection of the rotor collective angle would create a higher spectrum for the vertical velocity. Figure 19 illustrates this outcome by showing that the PSDs of the input are not affected by changing the number of blades of the rotor. This outcome aligns with the findings observed in the case of a single main rotor vehicle [8].

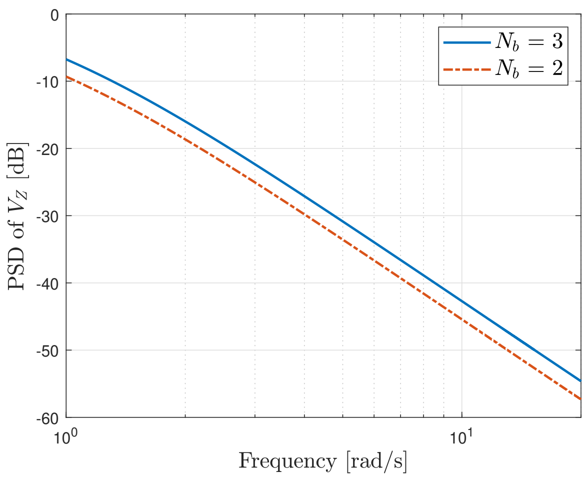

Figure 18: PSD of output: change of number of blades

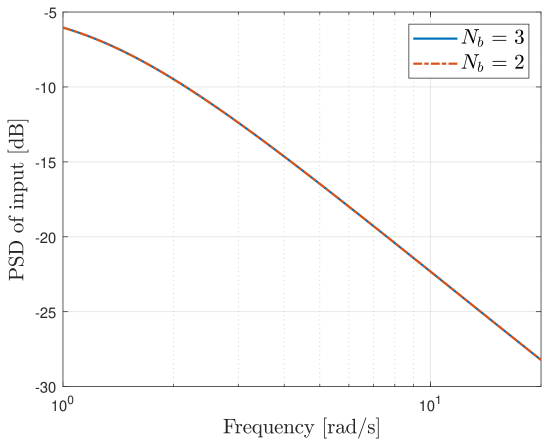

Figure 19: PSD of the input: change of number of blades

In the last phase, the chord length of the blades is altered (from a nominal value to 75% and 125% of the nominal value), and its impact on the RCETI model is observed. Since more surface area is exposed to turbulence when the chord length is larger, as is the case with more rotor blades, it is expected to observe higher spectra for the vertical velocity, as seen in Fig. 20. Furthermore, as in the case of the different numbers of rotor blades, the PSD of the input does not change significantly, as shown in Fig. 21, suggesting that the same RCETI model could be used to simulate the effect of vertical turbulence on rotor loads when changing the chord length of the rotor blades. The changes in both chord length and the number of rotor blades could potentially be combined as variations in rotor solidity (σ), although further examination is necessary.

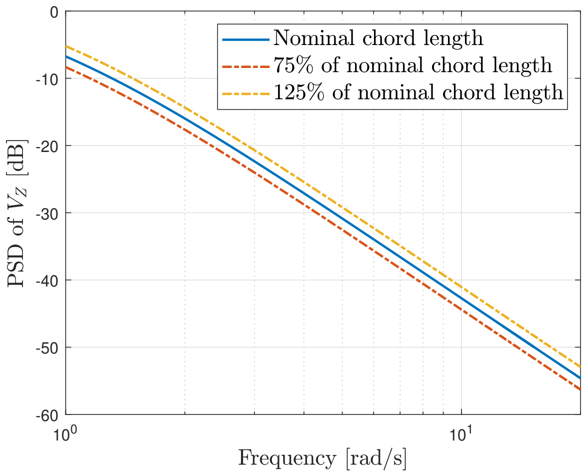

Figure 20: PSD of output: change of chord length

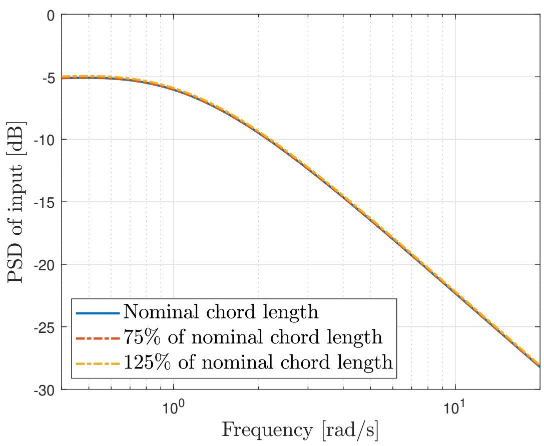

Figure 21: PSD of the input: change of chord length

4. CONCLUDING REMARKS

In this work, the concept of Rotor Control Equivalent Turbulence Input was applied to multi-rotor vehicles. A quadrotor model in FLIGHTLAB® was used. The heave axis response of the vehicle was studied as an example where the full vehicle was assumed to experience the same velocity fluctuations. This proves the assumption of using the same RCETI model on all of the rotors. In addition, different fluctuations of turbulence are also applied to the different rotors to study how the same RCETI model can effectively replicate the vehicle response. The following conclusions can be drawn from this work:

1. RCETI models can be created using the rotor inputs (rotational speed or pitch angle) to replicate the output spectrum caused by turbulence.
2. The rotor hub-loads can be employed as the outputs to which the spectrums are matched.
3. Utilizing a single RCETI model consistently across similar rotors within a multi-rotor vehicle yields response outputs that exhibit stochastic similarity to response due to turbulence.
4. When considering different turbulence fluctuations applied to distinct rotors, the uniform application of the same RCETI model remains feasible, albeit necessitating distinct white noise inputs contingent on the specific turbulence conditions for each rotor. This demonstrates the adaptability of the RCETI approach to varying turbulence scenarios across different rotors.
5. Similar results of the difference between the CETI and the RCETI models are observed when using either the rotor rotational speed or collective angle as input.
6. For the case of vertical turbulence, similar to the case of a single main rotor, the same RCETI model may be applied with varying rotor parameters such as the number of blades or the chord length.

Future work will include studying the applicability of the RCETI models on multi-rotor vehicles for the longitudinal and lateral axes. In addition, the applicability of these RCETI models will be studied for different types of multi-rotor vehicles.

5. ACKNOWLEDGMENTS

This research was partially funded by the U.S. Government under Cooperative Agreement No. W911W6-21-2-0001. The U.S. Government is authorized to reproduce and distribute reprints for Government purposes notwithstanding any copyright notation thereon.

The views and conclusions contained in this document are those of the authors and should not be interpreted as representing the official policies of position, either expressed or implied, of the U.S. Army Combat Capabilities Development Command (DEVCOM), Aviation & Missile Center (AvMC), or the U.S. Government.

REFERENCES

[1] Anon., "Flying qualities of piloted aircraft," *Dept. of Defense Interface Standard TR*, February 2006.

[2] G. Gaonkar, "Review of turbulence modeling and related applications to some problems of helicopter flight dynamics," *Journal of the American Helicopter Society*, vol. 53, pp. 87–107, 01 2008.

[3] J. Lusardi, C. Blanken, and M. Tischler, "Piloted evaluation of a uh60 mixer equivalent turbulence simulation model," 11 2002.

[4] S. W. Baillie and J. M. Morgan, "An in-flight investigation into the relationships among control sensitivity, control bandwidth and disturbance rejection bandwidth using a variable stability helicopter.," in *Proceedings of the 15^{th} European Rotorcraft Forum*, September 12-15 1989.

[5] J. Lusardi, *Control equivalent turbulence input model for the UH-60 helicopter*. PhD thesis, University of California, Davis, Jan. 2004.

[6] S. Seher-Weiss and W. Grünhagen, "Development of ec 135 turbulence models via system identification," *Aerospace Science and Technology - AEROSP SCI TECHNOL*, vol. 23, 12 2012.

[7] M. A. Hayajnh and J. V. R. Prasad, "Rotor control equivalent turbulence input (rceti) models," in *Proceedings of the 48^{th} European Rotorcraft Forum*, September 5-8 2022.

[8] M. A. Hayajnh and J. V. R. Prasad, "Development of parametric rotor control equivalent turbulence input (rceti) models for rotorcraft," in *Proceedings of the Vertical Flight Society 79^{th} Annual Forum*, May 16-18 2023.

[9] I. Advanced Rotorcraft Technology, *FLIGHT- LAB X-Analysis user manual*. 2013.

[10] S. Seher-Weiß and M. Jones, "Control equivalent turbulence input models for rotorcraft in hover and forward flight," *Journal of Guidance, Control, and Dynamics*, vol. 44, no. 8, pp. 1517–1524, 2021.

[11] T. Berger and M. J. S. Lopez, "Frequency domain identification of a multi-input control equivalent turbulence input model," *Journal of Guidance, Control, and Dynamics*, vol. 45, no. 1, pp. 15–27, 2022.

[12] A. G. P. Julius S. Bendat, *Random Data: Analysis and Measurement Procedures*, ch. 5. Wiley, 4th edition ed., 2010.

[13] M. Tischler and R. Remple, *Aircraft and Rotorcraft System Identification: Engineering Methods with Flight Test Examples*. AIAA education series, American Institute of Aeronautics and Astronautics, 2012.

[14] D. A. Peters, D. D. Boyd, and C. J. He, "Finitestate inducedflow model for rotors in hover and forward flight," *Journal of the American Helicopter Society*, vol. 34, no. 4, pp. 5–17, 1989.

[15] R. E. McFarland and K. Duisenberg, "Simulation of rotor blade element turbulence," *NASA Technical Memorandum 108862*, January 1995.

[16] R. G. Lee and S. J. Zan, "Unsteady aerodynamic loading on a helicopter fuselage in a ship airwake," *Journal of the American Helicopter Society*, vol. 49, no. 2, pp. 149–159, 2004.

[17] G. I. Taylor, "The spectrum of turbulence," *Proceedings of the Royal Society of London. Series A - Mathematical and Physical Sciences*, vol. 164, no. 919, pp. 476–490, 1938.